Alternative Augmented-Plane-Wave Technique: Theory and Application to Copper

Dale Dean Koelling*
Magnetic Theory Group, Physics Department, Northwestern University, Evanston, Illinois 60201
(Received 16 February 1970)

An alternative augmented-plane-wave (APW) method based on the matching of both the function and derivative across the APW sphere boundary is presented. This matching is accomplished by expanding the basis function inside the sphere using two sets of functions for each l: One set consists of the solutions with zero derivative, and the other of those with zero value at the APW sphere surface. The method is then applied to the Chodorow copper potential as a test case. In addition, the relativistic formulation and the extension to include non-muffin-tin potential terms are presented.

I. INTRODUCTION

The basic concept of the augmented-plane-wave (APW) method is the joining of an atomiclike function close to the nuclei (inside the APW spheres) onto a plane wave in the "outer regions" of the unit cell (outside the APW spheres). These APW functions are then used as a basis set for a variational calculation. There are, however, two distinct approaches to the construction of this basis set arising from the impossibility of both satisfying the radial equation inside the APW spheres *and* matching onto a single plane wave. Slater[1] originally chose to satisfy the radial equation,[2] and this is the standard form of the APW method in use today. Using this basis set, the variational quantity is not unique[3] but provides a very useful technique. Slater and Saffren[4,5] later investigated the alternate approach of matching the solutions exactly. The resulting procedure was found to be harder to carry out than the original procedure.[6] It was shown to be equivalent to the earlier method,[5] and now has fallen into disuse. Bross[7] has considered a procedure which uses a "well-chosen" logarithmic derivative. The procedure to be described here is similar to the approach of Bross differing principally in that two well-chosen logarithmic derivatives are used instead of just one.

Schlosser and Marcus[8] have considered a procedure where one merely expands the functions inside and outside the spheres and allows each to vary independently since the properly formulated variational principle must result in the correct continuity conditions for the resulting trial function. Marcus[9] has also examined in great detail the full range of the nonuniqueness observed by Leigh[3] as well as considered a number of ways that one can augment the plane waves.[10]

The method described in this paper is another approach obtained by focusing on the continuity conditions at the APW sphere radius. This alternative APW method (AAPW) has in common with all the above-mentioned APW methods, as well as the various OPW methods proposed,[11] the use of the energy-variational formalism.[12] Therefore, what is actually being sought is a prescription for setting up a set of basis functions in which to expand the trial function. The prescription to be discussed in this paper is based on the (truncated) expansion of the radial function inside the APW spheres in the following two sets of functions, u_n^l and v_μ^l, defined by being a solution to the radial equation and satisfying the boundary conditions

$$u_n^l(R_s) = 0, \quad \frac{d}{dr}\, u_n^l(R_s) \equiv 1 , \tag{1a}$$

$$v_\mu^l(R_s) \equiv 1, \quad \frac{d}{dr}\, v_\mu^l(R_s) = 0 \tag{1b}$$

at the sphere radius R_s. Obviously, the matching of the radial function at the APW sphere boundary is easily done using these functions for each l.

The clue that the use of these functions will be useful is found by examining the d bands. In the standard APW calculations, these bands occur a few tenths of a Rydberg below the asymptote in the logarithmic derivative, that is, just below the energy of one of the u functions. The usual APW procedure demands that one matches the almost zero function onto the very finite spherical Bessel function. The result is that the convergence is slower for the d bands and that numerical accuracy is difficult to obtain. The AAPW procedure can be viewed as something in the spirit of the tight-binding scheme of Lafon.[13] Lafon takes atomic functions and then joins them to Gaussian functions at large radii to form his tight-binding basis functions. The AAPW scheme involves taking the u and v functions, which are solutions for a finite muffin-tin sphere, and joining them onto plane waves. One might expect that this would improve the convergence for d bands and it does. Furthermore, one no longer must keep a set of functions for each star as in the Saffren and Slater[4,5] procedure used by Howarth.[6]

The formalism required to apply the procedure to a muffin-tin potential is described in Sec. II. In Sec. III, the small modifications necessary to apply the method to non-muffin-tin potentials are discussed. A test application of the method to the Chodorow potential used by Burdick is described in Sec. IV. In Sec. V, the possible usefulness of this approach is discussed along with its relative advantages and disadvantages.

II. AAPW METHOD

The basis functions for the standard APW method are formed by joining continuously for each l the radial function (of given energy E) inside the spheres onto the spherical Bessel function of the plane wave outside the spheres. This leaves one with a discontinuous slope which leads to the presence of the logarithmic derivatives in the secular equation. This prescription works well except near the energies where for some l a node of the radial function occurs at the sphere radius R_s. Then one is trying to join a radial function which is zero onto a very finite spherical Bessel function of the plane wave. This shows up as an asymptote in the secular equation resulting from the asymptote in the logarithmic derivatives. The AAPW method is designed to avoid this difficulty by matching both the radial function and its derivative at the sphere radius R_s.

To set up the basis function corresponding to the plane wave with $\vec{k}$ vector

$$\vec{k}_i = \vec{k} + \vec{K}_i \quad , \tag{2}$$

it is necessary to construct the radial functions satisfying the following relations:

$$w_l(k_i, r, E) = \sum_n c_n^l(k_i) u_n^l + \sum_\mu d_\mu(k_i) v_\mu^l \, , \tag{3a}$$

$$\sum_n c_n^l(k_i) = \frac{d}{dr} j_l(|k_i| R_s) , \tag{3b}$$

$$\sum_\mu d_\mu^l(k_i) = j_l(|k_i| R_s) \, . \tag{3c}$$

As this is not a unique prescription for $w_l(k)$, the requirement that

$$\delta \langle w_l | H - E | w_l \rangle = 0 \tag{4}$$

be satisfied using a truncated expansion with N u functions and M v functions is also imposed. This is to be done by a Rayleigh-Ritz variation using two Lagrangian multipliers to satisfy (3b) and (3c). The normalization and overlap integrals required are

$$\int_0^{R_s} r^2 u_m u_n \, dr = A_n \delta_{nm} , \tag{5a}$$

$$\int_0^{R_s} r^2 v_\mu v_\nu \, dr = B_\mu \delta_{\mu\nu} , \tag{5b}$$

$$\int_0^{R_s} r^2 u_n v_\mu \, dr = R_s^2 / (E_\mu - E_n) \, . \tag{5c}$$

To formulate the variational procedure, the quantity

$$W = (c_n^l, d_\mu^l)[G^{-1}] \begin{pmatrix} c_n^l \\ d_\mu^l \end{pmatrix} + 2\lambda_1 \sum_n c_n^l + 2\lambda_2 \sum d_\mu^l \tag{6}$$

is defined with

$$[G^{-1}]_{nm} = \delta_{nm}(E_n - E) A_n \, , \tag{7a}$$

$$[G^{-1}]_{\mu\nu} = \delta_{\mu\nu}(E_\mu - E) B_\mu \, , \tag{7b}$$

$$[G^{-1}]_{n\mu} = [G^{-1}]_{\mu n} = \frac{R_s^2}{E_\mu - E_n} \left(\frac{E_\mu + E_n}{2} - E \right) . \tag{7c}$$

The matrix has been written as G^{-1} to point to the Green's-function nature of this development; G^{-1} will be singular for E chosen as an eigenvalue of the system. It is instructive to first assume G^{-1} nonsingular and obtain the solutions. Then one can consider the singular points. The variational requirements $\delta W = 0$ yield the result

$$\begin{pmatrix} c_n \\ d_\mu \end{pmatrix} = -G \begin{pmatrix} \lambda_1 \\ \lambda_2 \end{pmatrix} \, . \tag{8}$$

The Lagrange multipliers are determined by the conditions

$$\sum_n c_n^l = -\sum_n (\lambda_1 \sum_m G_{nm} + \lambda_2 \sum_\mu G_{n\mu}) = \frac{d}{dr} j_l(kR_s) , \tag{9a}$$

$$\sum_\mu d_\mu^l = -\sum_\mu (\lambda_1 \sum_m G_{\mu m} + \lambda_2 \sum_\nu G_{\mu\nu}) = j_l(kR_s) \, . \tag{9b}$$

Defining

$$\gamma_{uu} \equiv -\sum_{nm} G_{nm} \, , \tag{10a}$$

$$\gamma_{vv} \equiv -\sum_{\mu\nu} G_{\mu\nu} , \tag{10b}$$

$$\gamma_{uv} \equiv -\sum_{n\mu} G_{n\mu} = -\sum_{n\mu} G_{\mu n} , \tag{10c}$$

this yields

$$\lambda_1 = \left(\gamma_{vv} \frac{d}{dr} j_l - \gamma_{uv} j_l \right) \Big/ (\gamma_{uu}\gamma_{vv} - \gamma_{uv}^2) , \tag{11a}$$

$$\lambda_2 = \left(\gamma_{uu} j_l - \gamma_{uv} \frac{d}{dr} j_l \right) \Big/ (\gamma_{uu}\gamma_{vv} - \gamma_{uv}^2) \, . \tag{11b}$$

It is important to note that although G^{-1}, and thus G, depends on the energy E, it does not depend on the plane-wave $\vec{k}$ vector $\vec{k}_i$. Thus, as one would expect, the only way the k dependence enters the c_n^l and d_μ^l is through the spherical Bessel functions.

Returning to the case that G^{-1} is singular, one can no longer find G but there is still a solution which can be found using the eigenvalue-eigenvector decomposition of G^{-1}. However, there is a simple trick which can be used such that these special cases need not be treated as a special case.

The matrix G^{-1} is expanded by adding to rows and columns to construct the matrix Q^{-1} of the form

$$Q^{-1} = \left[\begin{array}{c|cc} & 1 \;\; 0 & \uparrow \\ & \vdots \;\; \vdots & \\ G^{-1} & & N \\ & 1 \;\; 0 & \downarrow \\ \hline & 0 \;\; 1 & \uparrow \\ & \vdots \;\; \vdots & \\ & & M \\ & 0 \;\; 1 & \downarrow \\ \hline 1\ldots10\ldots0 & 0 \;\; 0 & \\ 0\ldots01\ldots1 & 0 \;\; 0 & \end{array}\right] . \qquad (12)$$

$\leftarrow N \rightarrow \quad \leftarrow M \rightarrow$

The resultant matrix equation is now

$$Q^{-1}\begin{pmatrix} c_n^l \\ d_\mu^l \\ \lambda_1 \\ \lambda_2 \end{pmatrix} = \begin{pmatrix} 0 \\ 0 \\ d/drj_l \\ j_l \end{pmatrix} , \qquad (13)$$

where the first $(N+M)$ rows yield the variational expressions for $\delta W = 0$ and the additional two rows are an explicit writing out of the boundary conditions. Equation (13) can now be solved, as Q^{-1} will be nonsingular. This form of the variation is what one would get if one were to include the $(d/dr)j_l$ and j_l in the variational quantity and then also do the variation on the Lagrange multipliers. The solutions obtained for the coefficients are

$$c_n^l(k) = Q_{n,\,N+M+1}\frac{d}{dr}\,j_l(kR_s) + Q_{n,\,N+M+2}\,j_l(kR_s) , \qquad (14a)$$

$$d_\mu^l(k) = Q_{N+\mu,\,N+M+1}\frac{d}{dr}\,j_l(kR_s) + Q_{N+\mu,\,N+M+2}\,j_l(kR_s) . \qquad (14b)$$

The (unnormalized) basis functions are now defined as

$$(N_c\Omega)^{1/2} f(\vec{k}_i, \vec{r}, E) \equiv e^{i\vec{k}_i\cdot r} + 4\pi \sum_m e^{i\vec{k}_i\cdot\vec{R}_m}\Theta(\rho_m, R_s) \otimes \sum_L^{l_{\max}} i^l Y_L^*(\hat{k}_i)\, Y_L(\hat{\rho}_m)\Delta_l(k_i, \rho_m, E) ,$$

$$\Delta_l(k_i, \rho_m, E) = w_l(k_i, \rho_m, E) - j_e(k_i R_s) , \qquad (15a)$$

$$\vec{\rho}_m = \vec{r} - \vec{R}_m , \qquad (15b)$$

$$L = \{l, m\} , \qquad (15c)$$

where the $\vec{R}_m$ are the lattice sites and N_c is the number of unit cells with volume Ω. $\Theta(r, R_s)$ is the step function such that it is one for r less than R_s and zero for r greater than R_s. The sum on l is truncated at a fairly low $l_{\max}$. This is done because even for U($Z = 92$), the radial functions are very nearly the free-electron solutions for $l \geq 4$. Although this would mean that the radial function should be $j_l[r\sqrt{(E+V_0)}]$, it will be much more convenient to use $j_l(kr)$ implied in Eqs. (15). This involves "degrading" the basis function for the higher l's, but since they contribute only a very small factor to the matrix elements, it will cause only a small error – one which will be at least partially accounted for in the variational calculation.

This set of basis functions is used to expand a trial function and a second Rayleigh-Ritz variation leads to the secular problem

$$\det(M) = 0 , \qquad (16a)$$

$$M_{ij} = \langle f_i | H - E | f_j \rangle . \qquad (16b)$$

In atomic units the matrix elements are

$$M_{ij} = H_{ij} - EN_{ij} , \qquad (17a)$$

$$H_{ij} = k_j^2\delta_{ij} + V(\vec{k}_j - \vec{k}_i) + S(\vec{k}_j - \vec{k}_i)\textstyle\sum_l P_l(\hat{k}_i\cdot\hat{k}_j)G_l(i,j) , \qquad (17b)$$

$$G_l(i,j) = (4\pi/\Omega)(2l+1) \times\{[w_l(i)|H_l|w_l(j)] - [j_l(i)|H_l|j_l(j)]\}, \qquad (17c)$$

$$N_{ij} = \delta_{ij} + S(\vec{k}_j - \vec{k}_i)\textstyle\sum_l P_l(\hat{k}_i\cdot\hat{k}_j)F_l(i,j) , \qquad (17d)$$

$$F_l(i,j) = (4\pi/\Omega)(2l+1) \times\{[w_l(i)|w_l(j)] - [j_l(i)|j_l(j)]\} , \qquad (17e)$$

$$S(\vec{k}_j - \vec{k}_i) = \sum_{\vec{t}\ \text{in}\ \Omega} e^{i\vec{t}\cdot(\vec{k}_j - \vec{k}_i)} , \qquad (17f)$$

where the square brackets [ ] in Eqs. (17c) and (17e) indicate that only the radial integrations remain to be done. The structure factor, Eq. (17e), appears because the atoms are assumed to be equivalent. (It is pointed out in Appendix A that the relativistic version of this procedure is also easily written.)

It should be noted that the matrix element M has been broken up into the Hamiltonian matrix H and the overlap matrix N. Besides making it easy to use the resultant trial functions for further calculations, this permits an alternative calculational procedure for finding the eigenvalues. One can

construct the matrices H and N separately. Then, from N, a triangular matrix is constructed (via the Schmidt orthogonalization procedure in matrix form) such that $U^{+}NU=1$. This transformation can be applied to H and the resultant matrix diagonalized, yielding a variational set of eigenvalues for the basis set constructed with the energy E as a parameter. One then chooses the eigenvalue of interest, constructs the matrices for E equal to that eigenvalue, and again repeats the process. This is continued until the used E and obtained eigenvalue agree to within the desired tolerance. This then is a self-consistency-type approach.

III. COMMENTS ON THE NON-MUFFIN-TIN POTENTIAL CASE

For any APW basis set, it is convenient to break up the crystal potential[14] as

$$V(\vec{r}) = V_m(\vec{r}) + V_1(\vec{r}) + V_2(\vec{r}), \tag{18}$$

where V_m is the muffin-tin approximation[15,16] to $V(\vec{r})$. V_1 is the difference between $V_m(\vec{r})$ and $V(\vec{r})$ in the region outside the spheres and V_2 is the difference inside the spheres.

It is now easily seen how the basis set is to be defined. One merely uses V_m to create the basis set as in Sec. II. Furthermore, if $V_2(\vec{r})$ is negligible, then the extension to a non-muffin-tin potential is quite straightforward: The $V(\vec{K})$ in Eq. (17b) now must be the Fourier component of the entire potential instead of just the muffin-tin part.

There are a number of materials where V_1 must be included and V_2 not be needed. After all, V_2 is defined in the region "close to" the nucleus where the atomic effects are expected to dominate. When it is necessary to include V_2, then it must be expanded in spherical harmonics or some combination thereof; thus,

$$V_2(\vec{r}) = \sum_L V_2^L(r)\, Y_L(\hat{r}) \quad . \tag{19}$$

Several of these $V_2^L \equiv 0$ because of the symmetry of the crystal.

In addition, $V_2^L(r)$ will only be of sufficient size to be of interest "near" the APW sphere surface. The higher the l, the more pronounced this will be. But in the region near the surface, the trial functions deviate only slightly from the Bessel function to which they were matched. This would imply that the most important feature to include is $V_2(\vec{K})$ – the plane-wave matrix element. The next part of the matrix element to be included is $(w_l - j_l)$ with a $(w_{l'} - j_{l'})$. In all likelihood, one could omit the matrix element of a $(w_l - j_l)$ with the higher l valued Bessel functions without appreciable error. Then one would need only the Fourier components of V_2 and a few radial integrals to adequately deal with the nonspherical potential V_2.

The general treatment of the nonspherical potential is notationally complex but logically straightforward. It need not be discussed here since the primary objective of this section has been merely to indicate that just as is the case for the standard APW technique,[14] the AAPW is not limited to a muffin-tin potential.

IV. APPLICATION TO Cu

The proposed AAPW method can only be a useful calculational tool if the expansions used converge conveniently and rapidly. This can only be tested by actually using the method for performing a calculation on a known material. In the past, the two favorite test cases for testing calculational techniques have been Li[7,12] and Cu.[17–19] Cu is preferred as a more severe test because it has d bands and low-lying core states. Thus one can study the application of the AAPW method to both the tight-binding-like and the plane-wave-like bands, while at the same time checking that there is no difficulty of convergence to a core state (orthogonalization problems).

The Chodorow potential – obtained by copying the values given by Burdick[18] and interpolating onto a logarithmic mesh – was chosen for the test case. The energies and normalization integrals of the u_n^l and v_μ^l functions were then determined. These are shown in Table I. The indices n and μ were chosen to be the number of nodes *inside* the muffin-tin radius and all energies are measured relative to the "muffin-tin floor" so that the bands of interest lie in the range -0.1–1.0 Ry.

One feature of Table I which should be noted immediately is the very large values of the nor-

TABLE I. Energies and normalization integrals for the u_n^l and v_μ^l functions of the Chodorow potential.

l	(n,μ)	$E\mu$	$B\mu$	En	An
0	2	− 7.435 37	1907.587	− 7.428 02	366.778 9
0	3	− 0.146 09	4.307 26	2.576 74	1.766 00
0	4	6.229 06	5.121 86	12.068 60	0.465 62
0	5	18.152 47	5.864 92	26.145 91	0.233 087
1	1	− 4.504 80	426.709 6	− 4.479 21	135.434 7
1	2	0.561 48	3.940 46	3.698 87	1.513 93
1	3	7.384 49	5.473 35	13.147 29	0.459 24
1	4	19.121 21	6.093 04	26.931 69	0.236 82
2	0	0.129 01	16.713 29	0.463 68	23.105 41
2	1	2.208 33	4.297 33	5.749 55	1.278 05
2	2	9.312 86	6.301 73	14.694 39	0.477 10
2	3	20.245 80	6.643 82	27.497 30	0.255 71
3	0	2.970 56	3.459 48	6.586 98	1.434 58
3	1	9.702 46	6.969 58	14.410 80	0.578 54
3	2	19.207 56	7.199 93	25.614 46	0.305 85
4	0	5.099 55	2.947 25	10.275 30	0.820 14
4	1	14.654 39	6.255 77	20.717 96	0.384 75
4	2	26.757 11	6.848 17	34.407 61	0.225 70

malization integrals of the core orbitals. This is easily understood since they are expected to be predominantly inside the muffin-tin sphere with a very small value at the surface. But since one would also expect the mixing in of a basis function to depend roughly on the inverse of the normalization integral times the energy difference, the contribution of the core functions must be small in the energy range of interest. In the initial calculations, however, they were alternately kept and omitted to check if they indeed were negligible.

In Table II, some representative energy eigenvalues found by the AAPW technique are compared with those of other methods.[17,18] As can be seen, the agreement is quite good for the lower-energy eigenvalues where the number of AAPW's included provided adequate convergence. For the higher eigenvalues, the values found tend to be somewhat high indicating that more AAPW's should be included. However, there are at least two other possible causes of the differences: (a) The "Chodorow potential" used in these calculations was obtained by a four-point Lagrangian interpolation onto a logarithmic mesh from the data given by Burdick.[18] (b) The choice of basis functions is different. In that light, it is interesting to note that the variations of the AAPW results are roughly the same size as the variations between the KKR and APW results.

As mentioned in Sec. II, it is possible to set up the problem to use a self-consistent diagonalization technique (DIAG) rather than using the more standard process of plotting the determinant as a function of energy (DET). Both the DIAG and DET procedures are concerned with matching the energy used to construct the basis functions with the eigenvalue found. However, since it is of interest to determine the usefulness of the DIAG approach, the AAPW computer codes were set up to use it in addition to the more standard DET scheme. In this way we are actually investigating two things at once: (a) the applicability of the AAPW method and (b) the usefulness of the DIAG approach. This is clearly possible since the AAPW tests are concerned with convergence whereas the DIAG tests are concerned with relative computer times of the two procedures. Most of the specifically calculational details are presented in Appendix B for the interested reader.

TABLE II. Results for the Chodorow potential (units are millirydbergs).

State	Present work	APW (Ref. 18)	Korringa-Kohn-Rostaker (Ref. 17)
Γ_1	$(-105)^a$	$(-104)^a$	$(-104)^a$
$\Gamma_{25'}$	404	403	399
Γ_{12}	465	461	459
X_1	268	271	262
X_3	306	304	296
X_2	507	503	502
X_5	522	516	517
$X_{4'}$	815	804	819
L_1	269	268	265
L_3	399	401	395
L_3	519	505	504
$L_{2'}$	620	605	621

[a]The Γ_1 value is given relative to the muffin-tin constant potential. All other eigenvalues are given such that the energy of the Γ_1 state is the zero of energy.

It is instructive to look at one other result of the calculations for the Chodorow potential. In order to actually see how the DIAG procedure works and study the approach to self-consistency, one can plot the eigenvalues found as a function of the energy parameter used to construct the basis functions. Of course, on such a plot the self-consistent eigenvalues are to be found on a 45° line passing through the origin. Figure 1 shows such a plot for the high-symmetry points Γ and L. From the figure one sees that there are two quite distinct behaviors for the eigenvalue dependence on the energy parameter E. For the one type, there is almost no dependence at all so the plot is almost a horizontal line. These eigenvalues are found very near the energies $(\vec{k}+\vec{k}_n)^2$ and so are the plane-wave-like states. For the second type, the eigenvalue is found at the bottom of a very sharp dip. These are the tight-binding-like d states. It is therefore obvious that this differing behavior is a result of the region of the unit cell in which it is important to have the basis functions be a good approximation to the wave function. That is, for the nearly free-electron states, the solution is fairly insensitive to what one does inside the muffin-tin spheres. On the other hand, what is done inside the muffin-tin spheres is extremely important for the d states.

V. DISCUSSION AND CONCLUSION

This paper has presented an experimental study of one of the many possible ways to construct a set of basis functions for a variational calculation of the energy bands in solids. Since all calculational methods currently in use are only marginally practical for the study of the more complex materials with lowered symmetry and/or multiple atomic constituents, it is imperative that such studies continue.

The AAPW method has some very desirable features to recommend it: (a) The asymptote problem no longer occurs as it does in the standard APW method. This can be of considerable importance when studying compounds where it is

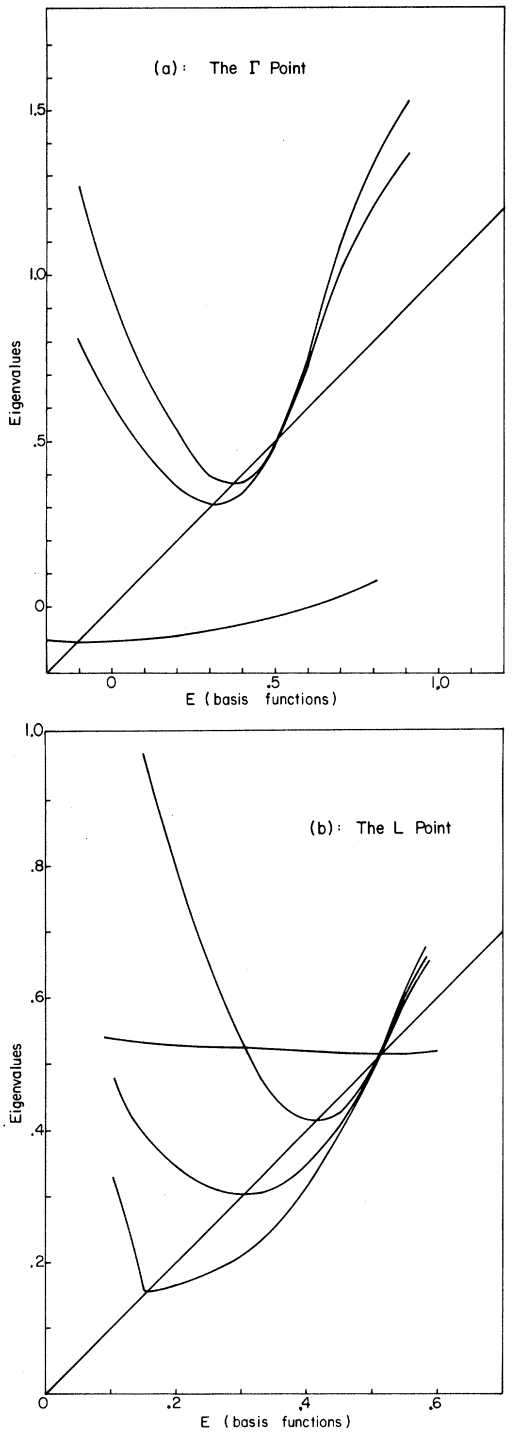

FIG. 1. Plot of eigenvalues found as a function of the variational energy parameter.

possible for more than one asymptote to occur in the energy range of interest. In such a case, it is very significant that the AAPW is far less susceptible to numerical errors in these regions than the standard APW method. (b) The normalization of the trial function is more conveniently obtained. This facilitates $\vec{k}\cdot\vec{p}$ approaches as well as calculations of other quantities requiring a knowledge of the wave function. (c) The atomic-sphere data appear in the calculation as only a few numbers (see Table I) instead of a tabulated set of logarithmic derivatives. Hence small adjustments of these data to correct for uncertainties in potential are very conveniently accomplished. Furthermore, if one parametrizes the Bessel function integrals of the potential, one can use this approach as an interpolation scheme. (d) The relativistic generalization of this method is no more difficult than for the standard APW method. Therefore, the high Z materials can easily be included in the range of applicability of this method.

In order that this method be useful in the higher Z compounds for which it was originally intended, it will be necessary to use linear combinations of AAPW's as basis functions in order to decrease the size of the secular determinant to a more manageable size. These combinations can be either those dictated by symmetry (i.e., a symmetrized formulation) or a more general combination based on a knowledge of the actual solutions at a given $\vec{k}$ point (i.e., an approach much in the spirit of the $\vec{k}\cdot\vec{p}$ method although no momentum matrix elements would be calculated). This additional sophistication requires a much more complex computer program than the simple test routine which has been used for these calculations. Such a program is presently under construction.

ACKNOWLEDGMENTS

The author is grateful to Dr. A. J. Freeman and Dr. F. M. Mueller for several valuable discussions. The programming assistance of Miss Susanna Katilavas and David Deford is gratefully acknowledged. Part of this work was done as a visitor to the Argonne National Laboratory.

APPENDIX A: RELATIVISTIC MODIFICATION

To obtain the relativistic formulation, the Foldy-Wouthusen transformed Dirac formalism will be used as has been done[20] for the standard relativistic-augmented-plane-wave (RAPW) technique. In the regions where the potential is "weak" such as in the region outside the APW spheres, this will yield

$$\phi_{FW}=\begin{pmatrix}\phi^{u}_{\mathrm{Dir}}\\ 0\end{pmatrix}+\frac{(E-V)}{2mc^2}\begin{pmatrix}\phi^{u}_{\mathrm{Dir}}\\ \phi^{v}_{\mathrm{Dir}}\end{pmatrix}+O\left[\left(\frac{E-V}{mc^2}\right)^2\right]. \tag{A1}$$

The factor $(E-V)/mc^2$ will be of order 10^{-4} in the region outside the spheres so one can without appreciable error use Pauli spinors in that region with a Schrödinger equation. Since the normaliza-

tion is not important at this stage, the basis functions can be chosen as

$$\phi_{FW}(\vec{k}, s; \vec{r}) = \begin{pmatrix} \chi^s \\ 0 \end{pmatrix} e^{i\vec{k}\cdot\vec{r}}, \tag{A2}$$

where χ^s is the usual two-component spinor quantized along an axis.

To simplify the boundary matching problem, it will be convenient to introduce the function

$$X_\kappa^s(\hat{k}, \hat{r}) \equiv 4\pi \sum_\mu C(jl\tfrac{1}{2}; \mu s)\, Y_l^{\mu-s*}(\hat{k})\chi_\kappa^\mu$$

$$= \sum_{s'} D_\kappa(\hat{r}s'; \hat{k}s)\chi^{s'}, \tag{A3}$$

where χ_κ^μ is the central field spinor and

$$D_\kappa(\hat{r}s'; \hat{k}s) = 4\pi \textstyle\sum_\mu C(jl\frac{1}{2}; \mu s')\, Y_l^{\mu-s'}(\hat{r})\, Y_l^{\mu-s*}(\hat{k}), \tag{A4a}$$

$$D_\kappa(\hat{r}s'; \hat{k}s) = \langle s' | \{ | \kappa | P_l(\hat{k}\cdot\hat{r}) + iS_\kappa P_l(\hat{k}\circ\hat{r})(\hat{r}\times\hat{k})\cdot\sigma \} | s\rangle . \tag{A4b}$$

These functions have the properties

$$\chi^s e^{i\vec{k}\cdot\vec{r}} = \textstyle\sum_k i^l(kr) X_\kappa^s(\hat{k}, \hat{r}), \tag{A5a}$$

$$\int d^2\hat{r}\, X_\kappa^{si}(\hat{k}_i, \hat{r})^\dagger X_\lambda^{sj}(\hat{k}, \hat{r}) = 4\pi\delta_{\kappa\lambda} D_\kappa(\hat{k}_i s_i; \hat{k}_j s_j) . \tag{A5b}$$

Throughout these expressions, κ is the relativistic quantum number and S_κ its sign. l and j are determined by the relations

$$j = |\kappa| - \tfrac{1}{2}, \tag{A6a}$$

$$l = |\kappa| + \tfrac{1}{2}(S_\kappa - 1) . \tag{A6b}$$

The basis function can now be defined as

$$(N\Omega)^{1/2} f(\vec{k}_i s_i, \vec{r}, E) = \begin{pmatrix} \chi^{si} \\ 0 \end{pmatrix} e^{i\vec{k}_i\cdot\vec{r}} + \textstyle\sum_m \Theta(|\vec{\rho}_m|, R_s) e^{i\vec{k}\cdot\vec{R}_n} \left\{ \sum_\kappa F \begin{pmatrix} g_\kappa X_\kappa^{si} \\ f_\kappa \sigma_r X_\kappa^{si} \end{pmatrix} - j_l(k_i|\vec{\rho}_m|) \begin{pmatrix} X_\kappa^{si} \\ 0 \end{pmatrix} \right\} \tag{A7}$$

where F is the Foldy-Wouthusen transformation operator. Now, of course, we want to join the upper component continuously and with continuous derivative to the Pauli spinor which we have in the outside the APW sphere with no concern about the small components. One can easily see that this is a reasonable procedure from (A1) since the surface of the APW sphere is a "nonrelativistic region."

By inserting these basis functions into the variational quantity constructed with the Foldy-Wouthusen transformed Hamiltonian and then performing the variation, one gets the secular equation

$$H_{ij} = \langle s_i | s_j\rangle [k_j^2\delta_{ij} + V(\vec{k}_j - \vec{k}_i)] + S(\vec{k}_j - \vec{k}_i) \textstyle\sum_\kappa G_\kappa(i,j) D_\kappa(\hat{k}_i s_i; k_j s_j), \tag{A8a}$$

$$G_\kappa = (4\pi/\Omega)\{[\kappa i | H_\kappa | \kappa j]_r - [j_l(i) | H_l | j_l(j)]\}, \tag{A8b}$$

$$N_{ij} = \langle s_i | s_j\rangle \delta_{ij} + S(\vec{k}_j - \vec{k}_i) \times \textstyle\sum_\kappa B_\kappa(i,j) D_\kappa(\hat{k}_i s_i; \hat{k}_j s_j), \tag{A8c}$$

$$B_\kappa = (4\pi/\Omega)\{[\kappa i | \kappa j]_r - [j_l(i) | j_l(j)]\} . \tag{A8d}$$

The r subscript on the brackets indicating a radial integral means that a four-component sum must also be performed. These integrals are done in the Dirac formalism as $F^\dagger F = F^{-1}F = 1$. Furthermore, these integrals are the only place where the relativistic effects enter as would be expected. Therefore the expressions in (A8) are the required result.

APPENDIX B: CALCULATIONAL CONSIDERATIONS

For the AAPW method, there are three convergence-related questions to be considered: (a) To what value $l_{\max}$ should one include the radial function w_l instead of the spherical Bessel function of the plane wave? (b) For each l, how many u_n^l and v_μ^l functions are to be used in the expansion of the radial function w_l? (c) How many AAPW's are to be used in any calculation? These convergence questions are the basis for the evaluation of the technique since they are merely a more specific way to ask how much computer time is necessary to perform a calculation.

The value of $l_{\max}$ chosen will affect the time required to set up the matrix in two ways. First, one must perform the radial Bessel function integral of the potential in Eq. (17c) for each of the $l_{\max}+1$ spherical Bessel functions. (There is an analytic expression for the Bessel function overlap integrals.) Second, one must set up and invert a matrix for each l to determine the coefficients of the w_l expansion. Thus it is desirable to keep $l_{\max}$ as small as possible, unlike the standard APW technique where adding the higher l radial functions costs virtually nothing in computer time. However, from experience with the RAPW[20] and self-relativistic-augmented-plane-wave (SRAPW)[21] methods, one can predict that an $l_{\max}=3$ should be most adequate for most metals (including Cu) if one remembers that the higher l radial functions are approximated as spherical Bessel functions instead of being just left out. Of course, $l_{\max}=2$ is the smallest value to be considered for Cu because of the d bands present. The value $l_{\max}=3$ was used in all calculations reported here and proved quite adequate.

If one uses $N u_n^l$ and $M v_\mu^l$ functions in the expansion of w_l, one must set up and invert an $(N+M+2)$-

dimensional matrix as well as perform the necessary coefficient manipulations in setting up the matrix. Since this must be done each time the energy parameter is changed, it is very desirable to truncate the expansion as rapidly as possible. Although the computer codes allow $M \neq N$, for the purposes of these tests M was always equal to N. This is approximately equivalent to expanding in "bands" since the energy of the v function will be slightly below an l-type band and the energy of the u function will be slightly above the l-type band. Furthermore, it was found that the best truncation procedure was based on the energy of the v functions as might be expected. A value of cutoff energy equal to 15 Ry was found to do quite well. This corresponds to using $N = 2$ for $l = 0$, $N = 2$ for $l = 1$, $N = 3$ for $l = 2$, and $N = 2$ for $l = 3$.

The number of AAPW's included will affect the time of the calculation by increasing the dimension of the matrix which must be diagonalized (or have its determinant evaluated). As this is the most time-consuming operation of the entire calculation (taking up roughly 95% of the calculational time in an SRAPW calculation, for example), it is important to choose the AAPW's included with great care. Furthermore, for n AAPW's one must perform $n(n+1)\ \frac{1}{2}(l_{\max}+1)$ spherical Bessel function integrals of the potential (17c). Although this is done only once for each $\vec{k}$ value, it does take time. To select the AAPW's which are to be used in the calculation, one makes the assumption that all AAPW's with $\vec{k}$ vectors of magnitude less than a given magnitude should be included. For the standard APW method, a rule of thumb has been developed[22] for the fcc and bcc crystals that $|k_{\max}|R_s = 5 + l_b$ for 0.001-Ry accuracy in a band of principally l_b (i.e., s, p, or d) character.[23] The calculations reported here have $|k_{\max}|R_s \leq 6.4$. Because of the limitations of the test program, it is not possible at this time to determine what level of convergence this represents although one would not expect the plane-wave convergence to differ radically from that of the standard APW method.

The DIAG and DET approaches were both used to test the usefulness of the DIAG approach. It was found that the DIAG approach was somewhat slower than the DET scheme for the application to Cu. In part, this was due to the fact that it takes roughly three to four times as long to perform a DIAG iteration as to evaluate a determinant. Using an improvement of the DET approach based on an observation made to the author by Williams,[24] it was still necessary to evaluate on the average two to three times as many determinants as diagonalizations to find an eigenvalue. Thus it would not take a tremendous improvement on the Householder-Givens diagonalization routine used for the DIAG procedure to match the speed of the DET scheme for cu. Therefore, in more closely spaced bands the DIAG scheme could have an advantage with the codes presently available to the author. And as it provides easy access to normalized trial (wave) functions, it is certainly a desirable procedure to maintain.

---

*Work supported by the Advanced Research Projects Agency through the Northwestern University Materials Research Center, Evanston, Ill. 60201.

[1]J. C. Slater, Phys. Rev. 51, 846 (1937).

[2]The trial function resulting from this expansion in functions with discontinuous slopes does have a continuous slope. See W. Rudge, MIT SSMTG Quarterly Progress Report No. 59, 1966 (unpublished), p. 8.

[3]R. S. Leigh, Proc. Phys. Soc. (London) A69, 388 (1956).

[4]J. C. Slater, Phys. Rev. 92, 603 (1953).

[5]M. M. Saffren and J. C. Slater, Phys. Rev. 92, 1126 (1953).

[6]D. J. Howarth, Phys. Rev. 99, 469 (1955).

[7]H. Bross, Phys. Kondensierten Materie 3, 119 (1964); H. Bross and H. Stohr, Phys. Letters 8, 25 (1964); H. Bross and H. G. Junginger, *ibid.* 8, 240 (1964).

[8]H. Schlosser and P. M. Marcus, Phys. Rev. 131, 2529 (1963).

[9]P. M. Marcus, Int. J. Quantum Chem. 1, 567 (1967).

[10]An important point not pointed out in Ref. 9 is that these terms result from the requirement that the variational operator be made Hermitian in the space of the basis functions used. This is actually a crucial point when one gets ready to do the relativistic generalizations of all these methods since this is most readily done using the Foldy-Wouthusen formalism. (The relativistic generalization of the AAPW method is presented in Appendix A.)

[11]A. B. Kunz, Phys. Letters 27A, 401 (1968); F. A. Butler, F. K. Bloom, and E. Brown, Phys. Rev. 180, 744 (1969); R. A. Deegan and W. D. Twose, *ibid.* 164, 993 (1967).

[12]W. Kohn, Phys. Rev. 87, 472 (1952).

[13]E. Lafon (private communication); see also, E. Lafon and C. C. Liu, Phys. Rev. 152, 579 (1966).

[14]P. De Cicco, Phys. Rev. 153, 931 (1967).

[15]L. F. Mattheiss, Phys. Rev. 133, A1399 (1964).

[16]F. S. Ham and B. Segall, Phys. Rev. 124, 1786 (1961).

[17]B. Segall, Phys. Rev. 125, 109 (1961).

[18]G. A. Burdick, Phys. Rev. 129, 138 (1963).

[19]J. S. Faulkner, H. L. Davis, and H. W. Joy, Phys. Rev. 161, 656 (1967).

[20]D. Koelling, Phys. Rev. 188, 1049 (1969).

[21]T. Loucks, Phys. Rev. 139, A1333 (1965).

[22]L. F. Mattheiss, J. H. Wood, and A. C. Switendick, in *Methods of Computational Physics* (Academic, New York, 1968), Vol. 8.

[23]This author, however, finds the rule to be somewhat optimistic.

[24]The author has found this observation extremely useful and wishes to express his gratitude for the discussion. The observation is simply that once one has performed the Gaussian elimination to obtain a triangular matrix, one can determine the number of eigenvalues below the energy E by counting the negative signs on the diagonal. This allows one to set up a procedure based on a wide mesh with subsequent iteration to find any number of eigenvalues which might occur with the mesh increment. From Fig. 1, one can see that there are some problems with this simple scheme, but none that cannot be dealt with.

PHYSICAL REVIEW B VOLUME 2, NUMBER 2 15 JULY 1970

High-Frequency dc Haas–van Alphen Oscillations in Aluminum†

J. R. Anderson and S. S. Lane*
Department of Physics and Astronomy, University of Maryland, College Park, Maryland 20742
(Received 16 February 1970)

High-frequency de Haas–van Alphen oscillations attributed to the second-zone Fermi surface have been studied in aluminum. The results have been combined with the lower-frequency values from the third-zone surface measured by Larson and Gordon in order to obtain a three-parameter pseudopotential-interpolation model. The parameters in Rydbergs are $V_{111}=0.018$, $V_{200}=0.062$, and $E_F=0.866_7$. This model has been used to calculate energy bands and a density of states.

I. INTRODUCTION

In recent years many experiments, including studies of the de Haas–van Alphen effect, [1–3] magnetoresistance, [4,5] magnetoacoustic effect, [6] cyclotron resonance, [7,8] and the Kohn effect, [9] have been undertaken in order to investigate the electronic structure of aluminum. These measurements have been consistent with a nearly free-electron Fermi surface. The simplest model of this surface, the single orthogonalized-plane-wave (OPW) or empty-lattice model, consists of three contributions: (i) a large second-zone hole surface (Fig. 1); (ii) a multiply-connected third-zone electron surface; (iii) small fourth-zone pockets of electrons. [10] A more realistic model is obtained by rounding the sharp corners of the empty-lattice model and eliminating the fourth-zone pockets. Detailed experiments, especially de Haas–van Alphen (dHvA) effect studies, have given a rather complete description of the third-zone surface. As shown by Ashcroft[11] a consistent description is obtained if this surface is no longer multiply connected but consists of separated toroid-like surfaces (Fig. 2).

The second-zone surface, however, has been much less completely investigated although ultrasonic attenuation[6] and Kohn effect[9] studies have suggested that the surface approximates the single OPW surface (Fig. 1). The only previous dHvA measurements on this surface have been the pulsed field measurements of Priestley[2] limited to magnetic field orientations along [110] and [111] symmetry directions. Since extremely accurate dHvA measurements are now possible and can be reliably interpreted, we decided to study the high-frequency dHvA oscillations in aluminum (4×10^8–6×10^8 G), related to the second-zone hole surface, and some intermediate frequencies resulting from the third zone. Our measurements combined with the low-frequency measurements of Larson and Gordon[3] have been used to obtain parameters for a four OPW interpolation model, [12] the same type of model as used by Ashcroft. [11]

Even higher-frequency oscillations (1×10^9–1.5×10^9G) have been observed at some orientations and are probably related to magnetic breakdown. Parker and Balcomb[5] observed strong oscillations in the magnetoresistance and suggested that these were due to breakdown between the small pieces of the third-zone surface and the large second-zone hole surface. The highest-frequency dHvA oscillations observed in this investigation have been interpreted in a similar manner.

II. EXPERIMENTAL TECHNIQUES

Measurements of the dHvA effect were made using the low-frequency modification of the field-modulation technique first described by Shoenberg and Stiles. [13] These measurements were normally made at the second harmonic of the 44.3-Hz fundamental frequency. A carefully constructed notch filter[14] (rejection about 80 dB per octave) was